GPS and Glonass in the ERA of Multi-GNSS: Signals, Modernization, and Positioning Accuracy

Kanat Zhunussov[1], Nurlan Kystaubayev[1], Almukhan Nuraliyev[2,3], Raxmatillo Karimov[3,4,a)], Muratbay Bekimbetov[5], Erkin Sabirov[2], Abror Isakov[6]

[1] *Satbayev University, Almaty, Kazakhstan*
[2] *"Tashkent Institute of Irrigation and Agricultural Mechanization Engineers" NRU, Tashkent, Uzbekistan*
[3] *Tashkent State Technical University named after Islam Karimov, Tashkent, Uzbekistan*
[4] *Almalyk State Technical Institute, Almalyk, Uzbekistan*
[5] *Karakalpak State University named after Berdakh, Nukus, Uzbekistan*
[6] *Academy of the Ministry of Internal Affairs of the Republic of Uzbekistan, Tashkent, Uzbekistan*

[a)] *Corresponding author:* raxmatillo82@mail.ru

Abstract. This article presents an analytical review of the modern global navigation satellite systems GPS and GLONASS, with emphasis on their architectural characteristics, signal structures, positioning accuracy, and integration capabilities within a multi-GNSS environment. Key modernization pathways of next-generation satellite platforms (GPS III/IIIF and GLONASS-K2) are examined, including the transition of GLONASS from FDMA to CDMA, the introduction of civilian signals L1C, L5, and L3OC, as well as improvements in atomic clocks and ephemeris models. A comparative analysis of signal characteristics, frequency bands, navigation message formats, time-synchronization schemes, and Signal-in-Space Range Error (SISRE) metrics is provided. Particular attention is given to high-precision positioning methods such as PPP, RTK, and PPP-RTK, as well as the role of global correction services (Galileo HAS, IGS MGEX, Trimble RTX). The results demonstrate that combining GPS and GLONASS significantly improves observation geometry, accelerates convergence, and enhances solution robustness, enabling centimeter-level real-time positioning. The analysis of development trends highlights the emergence of next-generation multi-GNSS architectures tailored for integration with INS, vision-based navigation, AI-supported processing, and digital geospatial infrastructures.

INTRODUCTION

Global Navigation Satellite Systems (GNSS) represent a key component of modern worldwide infrastructure for positioning, navigation, and time synchronization. Historically, the Global Positioning System (GPS), developed and maintained by the U.S. Department of Defense, has played a central role in enabling global spatial positioning, while Russia has simultaneously advanced its own navigation system, GLONASS. Over the past decades, both systems have undergone extensive modernization, including the deployment of new satellite platforms, the expansion of civilian signal sets, and the transition toward multi-system operation-significantly improving accuracy, reliability, and availability of positioning on a global scale [1-3, 6].

The current stage of GNSS development is characterized by two interconnected trends. The first trend involves the technical modernization of satellite constellations: the introduction of GPS III/IIIF and GLONASS-K/K2 satellites, the emergence of new civilian signals (e.g., L1C, L5, L3OC), and improvements in atomic clock stability and ephemeris accuracy. The second trend reflects the shift from single-system to multi-GNSS solutions, in which users and services simultaneously utilize signals from GPS, GLONASS, Galileo, and BeiDou to enhance positioning precision and robustness [4-6, 24]. The combined use of multiple constellations improves the geometric dilution of precision (PDOP), reduces the likelihood of solution outages under partial satellite visibility, and accelerates the convergence of high-precision positioning methods such as PPP and RTK.

The objective of this technical review is to provide a concise and informative comparison of the architectural and signal-level design choices of GPS and GLONASS, to assess modern approaches to achieving high accuracy (PPP, RTK, PPP-RTK, HAS), and to analyze their practical applicability in engineering contexts. Emphasis is placed on the technical aspects of modernization (new signal formats and frequency plans), on quantitative performance indicators (accuracy, SISRE, convergence time), and on multi-GNSS integration mechanisms (correction services, SSR/RTCM formats, and time-scale alignment) [7-9, 13].

The article is structured as follows. Section 2 provides an overview of the system architecture of GPS and GLONASS, highlighting differences and points of interoperability. Section 3 examines the signal structures and navigation message formats, comparing major frequency bands and modulation schemes. Section 4 discusses modern methods for achieving high-precision positioning (PPP, RTK, PPP-RTK, HAS) and presents system performance analysis. Section 5 explores GNSS interoperability and multi-system integration, including time-synchronization challenges and inter-system biases. Section 6 reviews current technological trends, such as integration with INS, AI, and IoT, as well as ongoing satellite modernization. Section 7 summarizes the main findings and provides recommendations for practical applications and future research.

Thus, this review is intended for specialists and engineers in satellite navigation and geodesy who require a concise, technically rigorous summary of contemporary advancements and practical approaches to the use of GPS and GLONASS in high-precision applications. The primary sources and empirical data used in this review include both foundational literature and recent studies on the performance evaluation and modernization of GNSS systems [1-9, 13].

ARCHITECTURE OF THE GPS AND GLONASS SYSTEMS

The architectures of GPS and GLONASS are generally similar and consist of three major segments: the space segment (satellite constellation), the ground control segment, and the user segment. Despite sharing a common conceptual structure, the systems were developed independently, resulting in several technical differences that influence their performance, accuracy, and interoperability.

Space Segment: The GPS space segment comprises 24-32 satellites distributed across six orbital planes with an inclination of 55^0 and an altitude of approximately 20,200 km. The current constellation includes GPS IIR-M, IIF, and GPS III satellites, which provide enhanced signal power, improved atomic clock stability, and modern civilian signals such as L1C and L5.

The GLONASS space segment traditionally consists of 24 satellites in three orbital planes with an inclination of 64.8^0 and an altitude of about 19,100 km. Earlier GLONASS-M satellites employed an FDMA-based signal structure, whereas the newer GLONASS-K and GLONASS-K2 generations implement CDMA modulation, the L3OC channel, and an extended set of frequency bands [10-15].

Differences in orbital parameters lead to distinct visibility geometries:

- the higher inclination of GLONASS enhances visibility at northern latitudes;
- GPS provides more uniform global coverage.

When combined within multi-GNSS solutions, this complementarity improves the Position Dilution of Precision (PDOP) by approximately 20-40%.

Ground Control Segment: The GPS ground control segment is operated by the Operational Control Segment (OCS), which includes monitoring stations, uplink facilities, and the Master Control Station. Its modernization under the OCX program has improved ephemeris accuracy and enabled support for new GPS III signals.

The GLONASS control system comprises the Main Information and Analytical Center (MIAC), measurement and correction stations, and a wide network of ground monitoring points. Recent upgrades include the deployment of new-generation ground stations and improved ephemeris-generation algorithms, reducing orbit prediction errors (SISRE) to the level of 0.6-0.7 m for K2 satellites [12].

User Segment: Modern GNSS receivers used in geodesy, autonomous transportation, and aviation commonly operate with multiple constellations-GPS, GLONASS, Galileo, and BeiDou. Key advances in the user segment include the adoption of:

- multi-frequency reception (L1/L2/L5);
- support for advanced signals (GPS L1C, L5; GLONASS L3OC);
- integrated GNSS+INS systems and AI-enhanced filtering techniques for improved robustness.

Key Architectural Differences: Despite their structural similarities, GPS and GLONASS exhibit several system-level differences that influence signal processing, performance, and interoperability. Table 1 summarizes the main architectural distinctions between the two systems.

TABLE 1. Main technical differences between GPS and GLONASS

Characteristic	GPS	GLONASS
Modulation type	CDMA	FDMA (M), CDMA (K/K2)
Orbital inclination	55°	64.8°
Frequency plan	Fixed	Offset (FDMA), fixed in K2
Signals	L1 C/A, L2 P(Y), L5, L1C	G1, G2, L3OC (modern)
Atomic clocks	Rubidium, Cs, H-masers (III+)	Cs, H-masers (K2)

Impact of architectural differences on performance.

Several of these differences have a measurable effect on positioning accuracy and consistency:

- the FDMA frequency plan introduces inter-frequency biases (IFB), which degrade PPP performance [15, 29-37];

- the transition to CDMA in GLONASS-K2 eliminates IFB and significantly improves interoperability with GPS [11-12, 16-28, 38].

New-generation signals of GPS III and GLONASS-K2 provide improved spectral uniformity and lower noise levels, enhancing tracking and phase stability [10-11, 21-23, 37-38].

SIGNAL STRUCTURE AND NAVIGATION MESSAGES OF GPS AND GLONASS

General Principles of GNSS Signal Formation: The primary function of satellite navigation signals is to provide users with the information required to compute space-time coordinates, including ephemerides (orbital parameters), clock corrections, satellite health status, and auxiliary system data. A GNSS signal is a radio-frequency waveform transmitted in the L-band (1-2 GHz), onto which two independent components are superimposed: a pseudo-random noise (PRN) code and a navigation message [1, 25-26].

Each satellite transmits a unique pseudo-random code (PRN), enabling the receiver to identify the satellite and isolate its signal from others within the constellation. When the receiver-generated PRN code aligns with the transmitted code, a correlation peak is produced, from which the pseudorange-the signal travel time multiplied by the speed of light-is derived [2, 35-36].

The modulation and frequency structure of GNSS signals are designed to ensure robustness against noise and multipath effects. Most systems employ phase shift keying (PSK), while more advanced navigation signals apply hybrid modulations such as Binary Offset Carrier (BOC), which enhances spectral separation and improves cross-system compatibility [3, 35-39].

An important measure of signal quality is the carrier-to-noise density ratio (C/N_0), expressed in dB-Hz. For civilian GPS signals, typical C/N_0 values lie in the range of 40–50 dB-Hz, whereas new CDMA-based signals from GLONASS-K2 can reach up to 53 dB-Hz, providing improved phase stability and higher positioning accuracy [4].

GPS Signals and Frequency Bands: The GPS system transmits navigation signals in three primary L-band frequencies-L1 (1575.42 MHz), L2 (1227.60 MHz), and L5 (1176.45 MHz)-which form the foundation of civilian and military navigation services [5]. The key characteristics of these frequency bands, including modulation types, signal structure, and code formats, are summarized in Table 2.

TABLE 2. Main frequency bands and signal characteristics of the GPS system

Band	Purpose	Main Signals	Modulation	Code Type
L1	Primary civilian and military	C/A, P(Y), L1C	BPSK(1), TMBOC	PRN (1023 chips)
L2	Military and precise civilian	P(Y), L2C	BPSK(1)	CM / CL
L5	High-accuracy navigation, aviation	L5 (I/Q)	QPSK(10)	10.23 MHz code

L1C Signal and the Transition to GPS III: With the introduction of the GPS III generation, the system deployed the new L1C signal, which uses TMBOC (Time-Multiplexed BOC) modulation-an advanced structure combining the benefits of BOC(1,1) and BPSK(1) to improve spectral separation and tracking robustness [6, 12-15, 34, 40-43]. As summarized in Table 2, L1C includes two components:

- L1Cp (Pilot);
- L1Cd (Data).

This pilot-data structure enhances tracking performance, especially under weakened signal conditions. Importantly, the L1C signal is interoperable with Galileo E1, enabling unified multi-GNSS processing.

L2C and L5 Signals: The L2C signal-also shown in Table 2-supports enhanced civilian positioning accuracy and consists of two sub-codes:

- CM (short message, 10 230 chips);
- CL (long message, 767 250 chips).

This dual-code architecture provides improved resilience to transmission errors and better tracking reliability [7].

The L5 signal (Table 2) is a high-power, wideband (20 MHz) navigation signal using QPSK(10) modulation. It delivers high accuracy (≈0.5 m) and is designed for safety-critical aviation applications. It is fully interoperable with Galileo E5a, enabling precise multi-GNSS combinations [8, 35-39].

GPS Navigation Messages: GPS navigation data are transmitted through three formats:

- LNAV (Legacy Navigation) - 50 bit/s, 25 pages, 12.5-minute update cycle;
- CNAV (Civil Navigation) - 25 bit/s, 300-bit blocks, CRC integrity control;
- CNAV-2 - used in GPS III L1C/L5 signals with ephemeris updates every 30 s [9].

The CNAV-2 format introduces new page identifiers (SV IDs), extended time fields, and an improved atmospheric model, increasing satellite orbit prediction accuracy to 0.02 m RMS [10].

Signals and Frequency Bands of the GLONASS System: Unlike GPS, the GLONASS system has historically been based on frequency-division multiple access (FDMA) [11]. The transition of GLONASS-K2 to a CDMA architecture and the introduction of the L1OC and L3OC signals significantly reduced inter-frequency biases and improved phase stability [34]. In the legacy FDMA configuration, each GLONASS satellite transmits on an individual carrier frequency. The L1 carriers are spaced around 1602 MHz, with each satellite assigned a slightly offset frequency according to its channel number, while the L2 carriers are centered near 1246 MHz with a similar offset scheme. The channel number k varies from -7 to +6, which leads to a set of discrete frequency slots across the constellation rather than a single shared carrier, as in GPS.

Beginning with the GLONASS-K generation, CDMA signals were introduced in the L3, L1, and L2 bands, marking a major step in system modernization. The modernization of civilian GPS and GLONASS signals has led to modulation alignment across systems-including TMBOC, BOC(1,1), and BPSK-which substantially improves interoperability in multi-GNSS receivers [33, 44-48].

TABLE 3. Frequency bands and signal characteristics of the GLONASS system

Band	Frequency (MHz)	Access Type	Modulation	Signal	Notes
L1	1602 ± k·0.5625	FDMA	BPSK	L1OF (legacy)	classical signal
L2	1246 ± k·0.4375	FDMA	BPSK	L2OF	military
L3OC	1202.025	CDMA	BPSK(10)	L3OC	new civilian signal
L1OC	1575.42	CDMA	BOC(1,1)	L1OC	interoperable with GPS L1C
L2OC	1248.06	CDMA	BPSK(10)	L2OC	interoperable with BeiDou B2a

New CDMA Signals and Performance Characteristics of GLONASS-K2: The transition to CDMA-based signals in the GLONASS-K and GLONASS-K2 generations represents one of the most significant steps in the modernization of the Russian navigation system. The introduction of the L3OC signal on GLONASS-K satellites marked the first fully open CDMA signal within GLONASS. L3OC employs BPSK(10) modulation with a 10 MHz bandwidth and a data rate of 100 bit/s, providing higher spectral efficiency and improved resistance to interference. Its received energy level is 2-3 dB higher than that of legacy FDMA signals, resulting in noticeably enhanced C/N_0 and reduced multipath sensitivity [12, 35-36, 44].

GLONASS-K2 further expands the CDMA signal set by adding L1OC and L2OC, designed to be interoperable with GPS L1C/L5 and Galileo E1/E5a. These signals use modern modulation schemes-BOC(1,1) and BPSK(10)-and feature separate Pilot and Data components to improve tracking robustness. They also transmit structured 600-bit navigation message blocks with a 2-second repetition cycle, aligning the system with current multi-GNSS messaging standards [13, 25-27, 33].

In terms of power and accuracy, GLONASS-K2 achieves performance levels comparable to modern GPS satellites. According to Thoelert (2024), the average received power of K2 signals reaches approximately −157 dBW, which is 4-5 dB higher than GLONASS-M. Correspondingly, the Signal-in-Space Range Error (SISRE) for GLONASS-K2 is 0.6-0.7 m, approaching the 0.45-0.5 m SISRE typical of GPS III [14, 36]. These improvements

indicate that the new GLONASS generation has effectively reached parity with GPS in both spectral quality and positioning accuracy.

Navigation Messages and Data Transmission: Navigation messages provide the essential information required to compute a precise user solution, including satellite coordinates, velocity, clock parameters, and a range of corrective terms. In the GPS system, the classical LNAV format is transmitted at 50 bit/s and features a rigidly structured organization: the complete data cycle consists of 25 pages grouped into five frames, each lasting 30 seconds, resulting in a 12.5-minute update period [15, 49-51].

Modern formats CNAV and CNAV-2 employ a packet-oriented structure containing 300-600-bit blocks, incorporate CRC-based integrity checks, and support more frequent ephemeris updates. These enhancements significantly improve the robustness and accuracy of the navigation solution under varying environmental conditions.

In the GLONASS system, the traditional FDMA-based L1/L2 message structure transmits 85-bit messages every 2 seconds at a rate of 50 bit/s. With the transition to a CDMA architecture in the GLONASS-K and GLONASS-K2 generations, the navigation message formats have become substantially more advanced. The L1OC, L2OC, and L3OC formats employ blocks of approximately 600 bits, transmitted at 100 bit/s, with ephemeris updates every 30 seconds [16]. Importantly, GLONASS-K2 navigation messages for the first time include signal integrity information and SISRE estimates, enabling improved reliability and suitability for high-precision and real-time applications.

Comparison of Signals and Frequency Bands: The comparative characteristics of GPS and GLONASS signals are summarized in Table 4, highlighting differences in modulation, frequency plans, navigation message structures, and interoperability across systems [8, 12-14, 17, 22, 35-37].

TABLE 4. Comparative parameters of GPS and GLONASS signals

Band	System	Frequency (MHz)	Modulation Type	Message Format	Data Rate	Compatibility
L1	GPS	1575.42	BPSK(1), TMBOC	LNAV, CNAV-2	50–100 bit/s	Galileo E1, BDS B1C
L2	GPS	1227.60	BPSK(1)	CNAV	50 bit/s	-
L5	GPS	1176.45	QPSK(10)	CNAV	100 bit/s	Galileo E5a
L1	GLONASS	$1602 \pm k \cdot 0.5625$	FDMA (BPSK)	Legacy	50 bit/s	-
L3OC	GLONASS-K	1202.025	BPSK(10)	CDMA (new)	100 bit/s	GPS L5, Galileo E5
L1OC	GLONASS-K2	1575.42	BOC(1,1)	CDMA	100 bit/s	GPS L1C, Galileo E1
L2OC	GLONASS-K2	1248.06	BPSK(10)	CDMA	100 bit/s	BeiDou B2a

The data in Table 4 show that both navigation systems utilize closely aligned carrier frequencies and increasingly similar modulation schemes. GPS and GLONASS exhibit significant spectral overlap in the L1 region (~1575 MHz) and the L3/L5 region (~1200 MHz), facilitating a high degree of interoperability in multi-GNSS receivers.

Furthermore, both systems have transitioned toward modern code structures-such as BOC (Binary Offset Carrier) and BPSK (Binary Phase Shift Keying)-as well as converging message formats (e.g., CNAV in GPS and L3OC Message in GLONASS). These developments simplify unified data processing and enhance overall receiver performance. The quality of GNSS signal reception is strongly influenced by antenna characteristics, multipath suppression capabilities, and bandwidth compatibility, which become particularly critical in challenging urban or obstructed environments [28].

Spectral characteristics of modern GPS and GLONASS signals are illustrated in Figure 1. It can be seen that GPS L1/L1C and Galileo E1 share the same central frequency of 1575.42 MHz, while GLONASS L1OC is located near 1602 MHz due to the legacy frequency-offset scheme. The frequency regions of GPS L5 (1176.45 MHz) and GLONASS L3OC (≈1202 MHz) also lie in close proximity, confirming the interoperability of next-generation multi-frequency positioning solutions [10-11, 29, 37, 49-51].

The figure illustrates the spectral shapes of the GPS L1, L1C, and L5 signals, as well as the GLONASS L1OC and L3OC signals, with corresponding modulation types indicated (BOC, TMBOC, QPSK, and CDMA). The close spectral proximity of GPS L5 and GLONASS L3OC, along with the identical nominal frequency shared by GPS L1C and Galileo E1, highlights the high level of unification among modern GNSS signals [10-11, 37, 52-53].

Time and Frequency Synchronization: Precise time-of-reception is essential for accurate coordinate determination, making time and frequency synchronization a critical component of GNSS operations. GPS employs the GPS Time (GPST) scale, which is aligned with UTC(USNO), whereas GLONASS operates on the GLONASS Time (GLONASST) scale, referenced to UTC(SU). Both time scales are coordinated through the Bureau International des Poids et Mesures (BIPM), and as of 2023, the deviation between them did not exceed 20 ns [17].

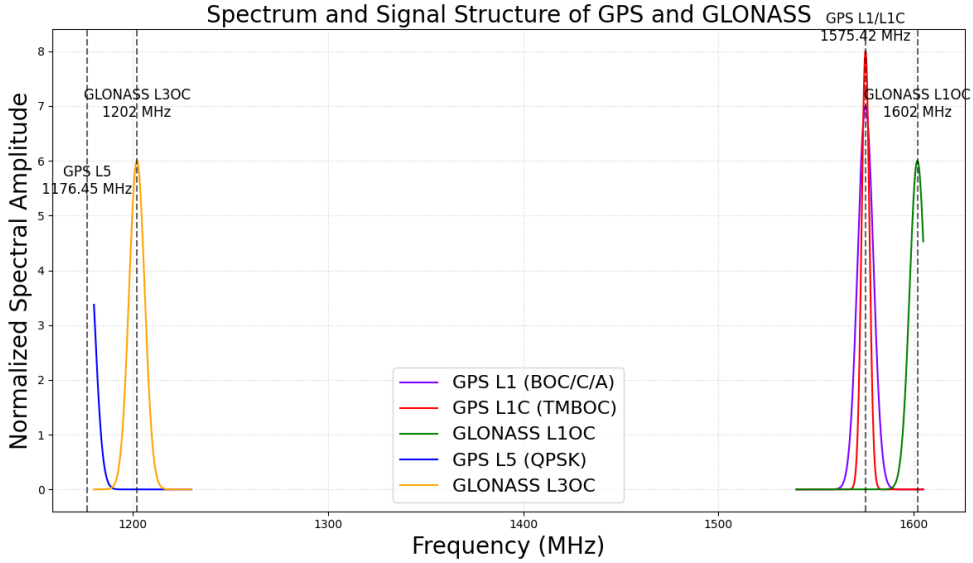

FIGURE 1. Spectrum and Structure of GPS and GLONASS Signals

Each satellite is equipped with highly stable rubidium or cesium atomic clocks operating at a stability level of 10^{-13}-10^{-14}, while the GLONASS-K2 generation incorporates hydrogen masers, improving long-term stability to approximately 10^{-15}. Such precise time synchronization is especially important for Precise Point Positioning (PPP) and for applications requiring high-accuracy time transfer (TT) between remote stations [18, 52-55].

POSITIONING ACCURACY AND PERFORMANCE OF GPS AND GLONASS

Positioning accuracy in GPS and GLONASS is determined by signal quality, atomic clock stability, ephemeris precision, and measurement characteristics. Modern GPS III and GLONASS-K2 satellites demonstrate significantly improved Signal-in-Space Range Error (SISRE), which directly enhances the performance of PPP and RTK techniques.

Error Sources and Factors Affecting Positioning Accuracy: The accuracy of GPS and GLONASS positioning solutions is influenced by a combination of orbital, clock, atmospheric, and hardware-related factors. Among these, the most critical are ephemeris errors and atomic clock instability, as they directly determine the magnitude of the Signal-in-Space Range Error (SISRE)-the key performance indicator of any GNSS constellation.

Modern GPS IIF and GPS III satellites achieve SISRE values of 0.3-0.6 m, whereas GLONASS-M satellites historically demonstrated slightly higher errors. The introduction of GLONASS-K and, in particular, GLONASS-K2 reduced SISRE to 0.5-0.8 m, bringing the performance of the Russian system to a level comparable with GPS in both PPP and RTK applications [10, 21, 29, 37, 55].

A distinctive factor affecting accuracy-especially in multi-frequency processing-is the presence of inter-frequency biases (IFB) in the legacy GLONASS-M system, caused by its FDMA signal structure. When GPS and GLONASS were used together in PPP solutions, these IFBs led to decimeter-level errors and significantly increased convergence time. The transition of GLONASS-K2 to a CDMA signal architecture completely eliminated IFB, making GLONASS fully interoperable with GPS, Galileo, and BeiDou at the physical signal level [11, 38, 42].

Improvements in signal characteristics, expanded bandwidth, and higher phase stability have significantly enhanced the precision of positioning, particularly in environments with limited satellite visibility. Recent studies confirm that GNSS accuracy is governed by the combined impact of orbital errors, clock instability, and reception conditions, requiring the use of extended correction models and advanced processing algorithms [27, 33-35].

Atmospheric effects also play a major role. Ionospheric delays introduce the largest contribution to pseudorange errors, while tropospheric delays manifest as slowly varying biases. Dual- and triple-frequency measurements effectively compensate for these effects, which is particularly important for PPP. With the expansion of available signals (L1/L2/L5 in GPS and L1OC/L2/L3OC in GLONASS-K2), the capability to mitigate atmospheric errors has improved substantially.

Performance of PPP, RTK, and Advantages of Multi-GNSS: High-precision positioning methods such as Precise Point Positioning (PPP) and Real-Time Kinematic (RTK) are essential tools for geodesy, autonomous systems, aviation, and scientific applications. GPS traditionally achieves high PPP accuracy, reaching 2–5 cm in the horizontal plane with convergence times of 15-40 minutes. Adding GLONASS increases satellite availability and improves observation geometry; however, in the FDMA era, legacy GLONASS signals limited the effectiveness of mixed-constellation PPP solutions.

With the transition to CDMA, the modernized GLONASS system provides stable carrier-phase observations, and PPP solutions using GPS + GLONASS exhibit significantly improved convergence and accuracy [21, 29, 37]. Comparative studies confirm that multi-GNSS processing substantially decreases RTK convergence time and enhances PPP robustness in environments with restricted satellite visibility [30, 49-51, 56-57].

RTK positioning-which relies on carrier-phase observations and real-time corrections from a base station or virtual reference station-achieves 1-2 cm accuracy for baselines up to 10 km. The inclusion of GLONASS increases the likelihood of rapid integer ambiguity resolution and reduces the probability of losing the fixed solution during short satellite blockages, which is especially important in urban canyons. Experimental analyses show that adding GLONASS increases RTK stability by 20-30% [10, 21, 58].

The comparison of PPP convergence times (Figure 2) shows that single-system GPS and GLONASS solutions typically require 30-40 minutes to reach a stable accuracy level, whereas multi-GNSS combinations reduce this interval to 10-20 minutes. These results are consistent with MGEX analyses and with performance assessments reported in Trimble RTX studies [21, 29, 37, 59].

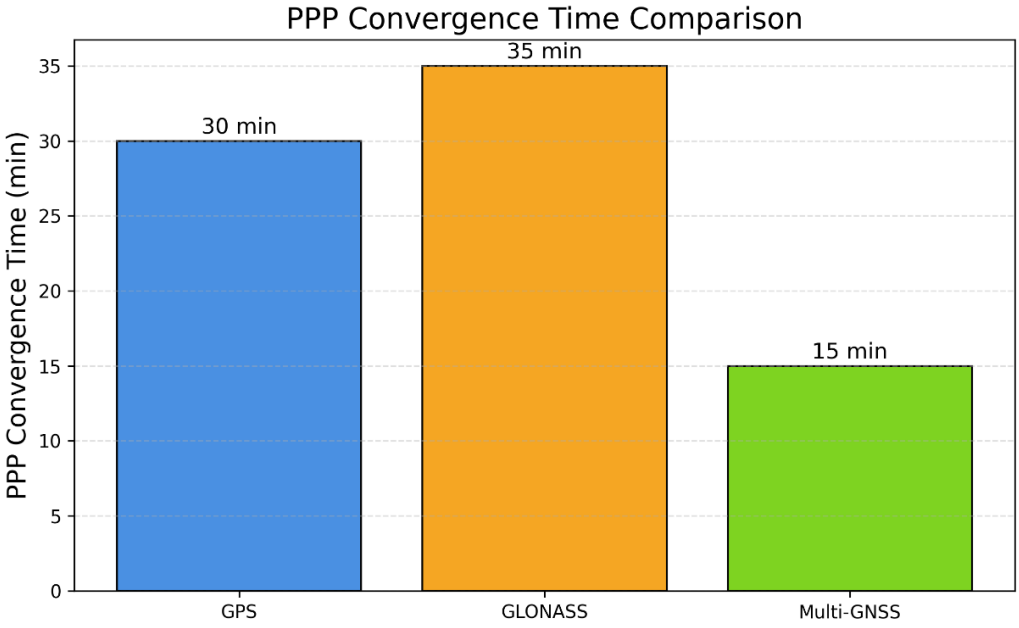

FIGURE 2. PPP Convergence Time for GPS, GLONASS, and Multi-GNSS

The use of combined observations significantly accelerates the achievement of centimeter-level accuracy, reducing convergence time by 40-60% compared with single-system solutions, as confirmed by experimental results from MGEX and Galileo HAS [21, 29, 59]. Multi-GNSS PPP-RTK, based on State Space Representation (SSR) corrections, demonstrates even higher performance. Services such as Galileo HAS, Trimble RTX, and IGS MGEX provide 2-5 cm accuracy with convergence times on the order of several minutes. The new CDMA signals of GLONASS-K2 make PPP-RTK involving GLONASS as stable and robust as PPP-RTK solutions built on GPS–Galileo combinations [37-38, 45-47].

Comparative Accuracy of GPS and GLONASS: A comparison of SISRE values for modern GPS III and GLONASS-K2 satellites is presented in Figure 3. GPS III achieves an average SISRE of approximately 0.45 m, whereas GLONASS-K2 demonstrates values around 0.65 m, which is consistent with orbit-error assessments reported by Montenbruck et al. and MGEX analyses [10, 29, 32, 37, 51-52].

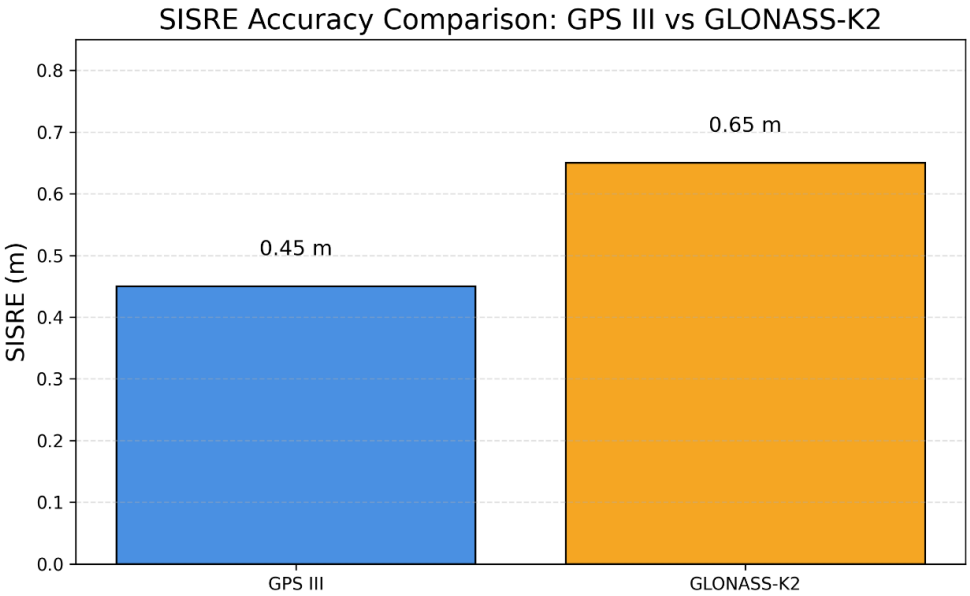

FIGURE 3. Signal-in-Space Range Error (SISRE): GPS III vs. GLONASS-K2

The figure presents a comparison of the average signal-in-space errors, highlighting the superior performance of GPS III in terms of atomic clock stability and ephemeris accuracy, as well as the substantial improvement achieved by GLONASS-K2 relative to earlier FDMA-based platforms [29, 37, 40, 60-61].

As summarized in Table 5, from the perspective of final positioning accuracy, both systems perform nearly equivalently when used within a multi-GNSS configuration.

TABLE 5. Key Quantitative Performance Parameters

Parameter	GPS III	GLONASS-K2
SISRE	0.3 – 0.6 m	0.5 – 0.8 m
PPP accuracy	2 – 5 cm	3 – 6 cm
Convergence time	15 – 25 min	20 – 30 min
RTK accuracy	1 – 2 cm	1 – 3 cm
Phase stability	high (L1C/L5)	high (L1OC/L3OC)

From the perspective of final positioning accuracy, both systems perform nearly equivalently when used within a multi-GNSS configuration.

Consolidated Conclusions on Accuracy and Performance: Modern satellite constellations-GPS III and GLONASS-K2-exhibit closely aligned accuracy levels and high stability of carrier-phase observations. The capabilities of multi-frequency positioning have expanded significantly in both systems due to the introduction of L1C, L5, and L3OC signals, which enhance atmospheric error mitigation and improve phase-tracking precision.

The use of multi-GNSS processing reduces PDOP, increases robustness under urban signal blockage, and shortens PPP-RTK convergence time. As a result, the combined use of GPS and GLONASS forms the backbone of high-precision navigation infrastructure and delivers essential benefits for autonomous systems, mapping, infrastructure monitoring, and scientific applications [10, 21, 29, 37, 38, 62-65].

The structure of error contributions is illustrated in Figure 4. For PPP, the dominant error sources remain orbit-clock errors and ionospheric delays, whereas for RTK the primary contributors are multipath and measurement noise. This distribution follows the classical GNSS error model, as documented in the foundational works of Misra & Enge and Montenbruck et al. [10, 21, 29, 37, 59].

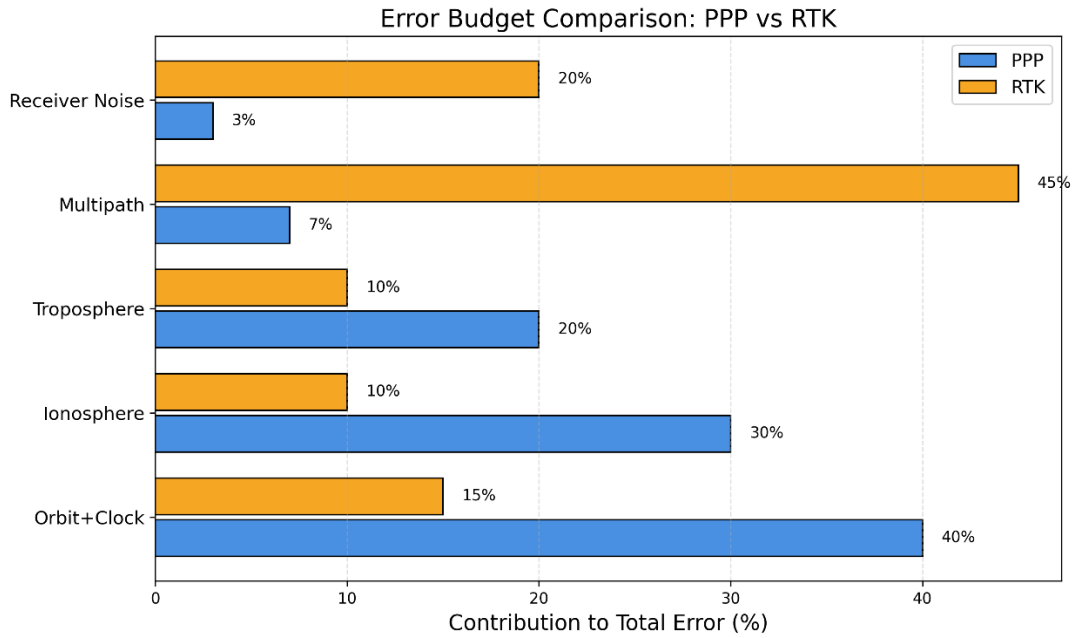

FIGURE 4. Error Structure in PPP and RTK Methods

The figure illustrates the relative distribution of key error components: PPP solutions are dominated by orbit-clock uncertainties and atmospheric delays, whereas RTK performance is primarily affected by multipath and environmental interference, especially in urban conditions. These patterns are consistent with MGEX studies and PPP-RTK performance analyses reported in modern high-precision services [21, 29, 41-44].

GNSS INTEROPERABILITY AND MULTI-SYSTEM INTEGRATION

Architectural Foundations of Multi-GNSS Integration: The modern navigation ecosystem is increasingly evolving toward multi-system integration, in which the GPS, GLONASS, Galileo, and BeiDou constellations operate as a unified positioning architecture. Combining observations from multiple systems significantly improves satellite geometry and thereby enhances positioning accuracy. In urban environments, dense infrastructure, or high-latitude regions, multi-GNSS solutions provide more stable performance due to the expanded set of available satellites and frequencies [10, 21].

Joint processing of measurements from different constellations leads to a notable reduction in PDOP and increases the robustness of carrier-phase observations, enabling accurate positioning even under partial sky visibility. Numerous studies demonstrate that this approach substantially improves the reliability and convergence speed of PPP and RTK methods, as additional frequencies and independent signals help suppress noise and resolve cycle ambiguities more effectively [29, 37, 41-42, 55].

Inter-System Time Scales and Biases: Despite the increasing unification of signal structures, multi-GNSS integration requires careful handling of discrepancies between the time scales of different systems. GPS Time does not include leap seconds, whereas GLONASS Time is synchronized with UTC(SU). Galileo System Time is aligned with TAI, while BeiDou Time maintains its own offset relative to GPST. These inconsistencies lead to inter-system time biases (ISB), which must be correctly modeled in PPP and RTK solutions [29, 37, 43, 61].

An additional source of systematic error in earlier generations of GLONASS was the presence of inter-frequency biases (IFB) caused by the FDMA modulation scheme. FDMA required frequency normalization and degraded carrier-phase observations in multi-frequency PPP solutions. The transition of GLONASS-K2 to a CDMA-based architecture eliminates IFB entirely, rendering the updated GLONASS configuration comparable in signal quality to GPS and Galileo [11, 38, 44, 56]. This development significantly improves the accuracy of mixed GPS+GLONASS PPP and RTK positioning.

Global High-Accuracy Services and Future Multi-GNSS Perspectives: One of the most significant recent advances has been the deployment of high-accuracy navigation services based on the State Space Representation

(SSR) concept. These services provide users with real-time orbital and clock corrections, integrity parameters, phase biases, and other data enabling centimeter-level positioning accuracy without local reference stations.

The Galileo High Accuracy Service (HAS) provides global coverage with 5-20 cm accuracy, whereas the commercial Trimble RTX service consistently delivers 2-4 cm results worldwide. The Japanese QZSS CLAS service targets regional high-accuracy positioning in Asia, achieving RTK-level performance. An additional source of high-precision corrections is the International GNSS Service (IGS), which provides open MGEX products supporting PPP and PPP-RTK solutions using all four major GNSS constellations [21, 29, 37, 45-46, 63].

The emergence of global correction services such as Galileo HAS enables real-time high-accuracy positioning using multi-frequency signals and standardized SSR formats [26, 47-48, 65].

Future developments in multi-GNSS architecture will be driven by ongoing modernization of satellite systems-including GPS III/IIIF and GLONASS-K2-expansion of frequency bands, improved atomic clock performance, and the introduction of new filtering algorithms based on inertial navigation systems, artificial intelligence, and 5G/6G connectivity. According to recent studies, PPP-RTK convergence times may be reduced to less than one minute in the coming years, while global real-time positioning accuracy is expected to approach the 1-2 cm level [11, 21, 49].

Thus, multi-GNSS integration is becoming a foundational technology for autonomous transportation, geodesy, aviation, and the emerging digital twin infrastructure of the Earth.

CURRENT TRENDS AND DIRECTIONS IN GNSS DEVELOPMENT

Transition Toward Real-Time High-Accuracy PPP-RTK Services: Recent years have been marked by rapid advances in high-accuracy positioning technologies based on the State Space Representation (SSR) concept. These services provide users with orbital, clock, phase-bias, and integrity corrections, enabling centimeter-level accuracy in real time without reliance on local reference stations. Among these solutions, the Galileo High Accuracy Service (HAS) has emerged as a key development, offering global coverage and near-RTK-level accuracy with reliable convergence within a few minutes [21, 50-51, 61-65].

Commercial services such as Trimble RTX provide even higher precision-typically 2-4 cm-along with highly stable performance across all continents [29, 52-53]. The combined use of PPP-RTK methodology with multi-GNSS observations significantly enhances robustness under limited satellite visibility and enables the achievement of sub-centimeter accuracy in real time.

Integration of GNSS with Inertial Systems, Visual Navigation, and Artificial Intelligence: A major trend in GNSS evolution is its deep integration with complementary sensory systems, including inertial measurement units (INS), cameras, lidars, and visual navigation algorithms. GNSS+INS fusion provides resilient positioning when satellite signals are partially or completely unavailable-such as in tunnels, urban canyons, indoor environments, or during highly dynamic maneuvers. Integrated GNSS–INS solutions ensure navigation continuity under signal outages and high-dynamics scenarios [19, 35, 44-47].

Integration with visual navigation systems has become essential for robotics, autonomous vehicles, and aerial platforms, as it combines the global accuracy of GNSS with the high-resolution local accuracy of visual methods [11, 25, 54]. Modern research shows that the inclusion of additional sensors-such as inertial units, BLE beacons, and visual systems-greatly improves accuracy and reduces reliance on satellite visibility [20].

Machine learning and deep neural networks are increasingly used to mitigate multipath, predict pseudorange errors, and optimize tracking-loop parameters, resulting in more stable phase measurements and significantly reduced PPP convergence times [30]. Regression-based and neural-network models further enhance GNSS reliability under signal blockage and multipath conditions and improve observation error prediction [22, 39].

GNSS Applications in IoT, Autonomous Transport, and Digital Infrastructure: The growth of the Internet of Things (IoT), autonomous transportation, and unmanned aerial systems has accelerated the development of compact and energy-efficient GNSS receivers capable of processing multiple constellations simultaneously. Modern consumer chipsets support GPS, GLONASS, Galileo, and BeiDou, providing 20-50 cm accuracy even without high-precision corrections.

In autonomous transportation, multi-GNSS plays a pivotal role in reliability and fault tolerance by increasing signal redundancy and improving trajectory estimation under challenging environmental conditions. On a global scale, GNSS forms the backbone of digital geospatial infrastructure required for digital twins of the Earth, infrastructure monitoring, transportation networks, agriculture, and scientific applications [21, 37, 51-55].

Hybrid GNSS solutions that combine satellite navigation with additional sensors and advanced filtering methods offer substantially improved positioning performance in dense urban environments and under dynamic motion [23].

In IoT applications, multi-GNSS combined with optimized positioning algorithms allows for reliable operation under restricted visibility and multipath-rich conditions [36].

Modernization of GPS III/IIIF and GLONASS-K2: A key developmental trend is the modernization of the GPS and GLONASS satellite constellations. GPS III satellites provide enhanced L1/L5 signal power, improved atomic clocks, and the new L1C civilian signal interoperable with Galileo E1. The upcoming GPS IIIF satellites will introduce high-gain directional antennas, reducing noise and increasing positioning precision.

GLONASS-K2 represents the first Russian platform fully transitioned to CDMA signals (L1OC and L3OC), eliminating inter-frequency biases characteristic of FDMA systems and making GLONASS fully interoperable with GPS, Galileo, and BeiDou at the signal-structure level [11, 38]. Improvements in orbital parameters and atomic clock stability have reduced SISRE and aligned system performance with GPS III.

Global Multi-GNSS Prospects Toward 2030: In the coming years, continued development of multi-GNSS infrastructure aims to enable global centimeter-level accuracy in real time. The expansion of the IGS MGEX network, deployment of new PPP-RTK services, and deeper integration of GNSS with 5G/6G networks and visual navigation will form the backbone of high-accuracy geolocation needed for autonomous transport, aviation, maritime navigation, and space missions.

According to expert assessments, PPP-RTK convergence times may be reduced to 10–60 seconds, while real-time accuracy may reach 1-2 cm, even in challenging environments [29, 37]. Current trends indicate a shift toward multi-frequency navigation, the expansion of high-accuracy correction services, and the growing role of multi-GNSS platforms in the global navigation ecosystem [37, 61-66].

Thus, multi-GNSS development represents a key trajectory in global navigation, shaping the future digital infrastructure of the Earth and enabling next-generation high-precision applications.

CONCLUSION

The conducted review demonstrates that the modern global navigation satellite systems GPS and GLONASS have reached a high level of technological convergence. Although historically different in their multiple-access principles and signal formats, both systems have undergone significant modernization, transitioning toward unified solutions in the L1 and L5/L3OC bands. This shift has enabled interoperability at the levels of frequency allocation, modulation, and navigation data structures. The transition of GLONASS-K/K2 to a CDMA-based architecture represents a critical milestone, eliminating inter-frequency biases and substantially improving phase stability and ephemeris accuracy. As a result, contemporary high-precision positioning methods-such as PPP, RTK, and hybrid PPP-RTK-achieve centimeter-level accuracy when GPS and GLONASS are used jointly, while multi-GNSS processing provides even greater robustness and reduced convergence times.

Analysis of Signal-in-Space (SISRE) parameters, atomic clock stability, and signal power confirms that the new satellite generations-GPS III/IIIF and GLONASS-K2-offer comparable performance, ensuring reliable positioning in environments with restricted visibility and challenging radio conditions. The review highlights promising future developments, including global correction services (Galileo HAS, IGS MGEX, and commercial PPP-RTK networks), expanded multi-frequency observations, improvements in navigation message quality, and enhanced inter-system compatibility.

The ongoing integration of GNSS with inertial navigation, visual navigation, radar systems, and machine learning algorithms forms the foundation of a new era of precision positioning required for autonomous transportation, unmanned systems, aviation, satellite geodesy, and digital twins of the Earth. Thus, GPS and GLONASS remain fundamental components of the multi-GNSS ecosystem, and their continued convergence and modernization will shape the quality and reliability of global navigation in the coming decades.

REFERENCES

1. O.Montenbruck, P.Steigenberger, J.M.Sleewaegen. *Data+ pilot biases in modern GNSS signals*. GPS Solutions. Vol. 27(3), (2023). P.112. https://doi.org/10.1007/s10291-023-01448-y

2. O.Montenbruck, P.Steigenberger, A.Hauschild. *Multi-GNSS signal-in-space range error assessment–Methodology and results*. Advances in Space Research. Vol.61(12), (2018). P.3020-3038. https://doi.org/10.1016/j.asr.2018.03.041

3. S.Thoelert, Steigenberger, O.Montenbruck. *GLONASS-K2 signal analysis*. GPS Solutions. Vol. 28(3), **141**, (2024). https://doi.org/10.1007/s10291-024-01681-z

4. P.Steigenberger, O.Montenbruck, *Characterization of the GLONASS-K1+ atomic frequency standard*. GPS Solut. Vol. 28, **196**, (2024). https://doi.org/10.1007/s10291-024-01736-1

5. Y.Lou, X.Dai, X.Gong, C.Li, Y.Qing, Y.Liu, ... S.Gu. *A review of real-time multi-GNSS precise orbit determination based on the filter method*. Satellite navigation. Vol. 3(1), **15**, (2022). https://doi.org/10.1186/s43020-022-00075-1

6. N.Nadarajah, A.Khodabandeh, K.Wang, M.Choudhury, P.J.Teunissen. *Multi-GNSS PPP-RTK: from large-to small-scale networks*. Sensors. Vol. 18(4), **1078**, (2018). https://doi.org/10.3390/s18041078

7. E.Ochin. *Fundamentals of structural and functional organization of GNSS*. In GPS and GNSS Technology in Geosciences. (2021), P.21-49. Elsevier. https://doi.org/10.1016/B978-0-12-818617-6.00010-X

8. E.Kaplan, C.Hegarty. *Understanding GPS/GNSS: Principles and Applications, 2017*. Boston, MA, Artech House. (2024).

9. P.S.Kumar, V.S.I.Dutt. *The global positioning system: Popular accuracy measures*. Materials today: proceedings. Vol.33, (2020), P.4797-4801. https://doi.org/10.1016/j.matpr.2020.08.380

10. W.Liu, B.Jiao, J.Hao, Z.Lv, J.Xie, J.Liu. *Signal-in-space range error and positioning accuracy of BDS-3*. Scientific Reports. Vol.12(1), (2022), P.8181. https://doi.org/10.1038/s41598-022-12012-y

11. J.Guo, X.Li, Z.Li, L.Hu, G.Yang, C.Zhao, ... M.Ge. *Multi-GNSS precise point positioning for precision agriculture*. Precision agriculture. Vol.19(5), (2018), P.895-911. https://doi.org/10.1007/s11119-018-9563-8

12. V.O.Zhilinskiy. *GLONASS Satellite Pseudorange Errors Mitigation Using Gradient Boosting Machine*. In 2021 XV International Scientific-Technical Conference on Actual Problems Of Electronic Instrument Engineering (APEIE). (2021), P.413-417. DOI: 10.1109/APEIE52976.2021.9647495

13. R.A.Sheikh, A.A.Al-Hadi, T.Sabapathy, H.Mirza, T.M.Hossain, P.Akkaraekthalin, P.J.Soh. *Review of Positioning Technologies and Antenna Designs for Indoor, Outdoor and Wearable Applications*. IEEE Access. (2025). DOI 10.1109/ACCESS.2025.3614190

14. Y.Shu, P.Xu, X.Niu, Q.Chen, L.Qiao, J.Liu. *High-rate attitude determination of moving vehicles with GNSS: GPS, BDS, GLONASS, and Galileo*. IEEE Transactions on Instrumentation and Measurement. Vol.71, (2022), P.1-13. DOI 10.1109/TIM.2022.3168896

15. B.Tan, Y.Yuan, Q.Ai, J.Zha. *Real-time multi-GNSS precise orbit determination based on the hourly updated ultra-rapid orbit prediction method*. Remote Sensing. 14(17), **4412**, (2022). https://doi.org/10.3390/rs14174412

16. D.Egea-Roca, M.Arizabaleta-Diez, T.Pany, F.Antreich, J.A.Lopez-Salcedo, M.Paonni, G.Seco-Granados. *GNSS user technology: State-of-the-art and future trends*. IEEE Access. Vol.10, (2022), P.39939-39968. DOI 10.1109/ACCESS.2022.3165594

17. S.Banu, H.Shanavas. *Ground Based Augmentation Systems (GBAS) with Global Navigation Satellite System (GNSS)*. In 2024 4th International Conference on Mobile Networks and Wireless Communications (ICMNWC). (2024), P.1-5. DOI: 10.1109/ICMNWC63764.2024.10872335

18. S.Cheng, F.Wang, G.Li, J.Geng. *Single-frequency multi-GNSS PPP-RTK for smartphone rapid centimeter-level positioning.* IEEE Sensors Journal. Vol.23(18), (2023), P.21553-21561. DOI 10.1109/JSEN.2023.3301658

19. Y.He, J.Li, J.Liu. *Research on GNSS INS & GNSS/INS integrated navigation method for autonomous vehicles: A survey.* IEEE Access, Vol.11, (2023), P.79033-79055. DOI 10.1109/ACCESS.2023.3299290

20. H.Luo, Y.Li, J.Wang, D.Weng, J.Ye, L.T.Hsu, W.Chen. *Integration of GNSS and BLE technology with inertial sensors for real-time positioning in urban environments*. IEEE access. Vol.9, (2021), P.15744-15763. DOI 10.1109/ACCESS.2021.3052733

21. Y.Zheng, F.Zheng, C.Yang, G.Nie, S.Li. *Analyses of GLONASS and GPS+ GLONASS precise positioning performance in different latitude regions.* Remote sensing. 14(18), **4640**, (2022). https://doi.org/10.3390/rs14184640

22. Q.Ai, K.Maciuk, P.Lewinska, L.Borowski. *Characteristics of onefold clocks of GPS, Galileo, BeiDou and GLONASS systems*. Sensors. 21(7), **2396**, (2021). https://doi.org/10.3390/s21072396

23. L.Zhu, H.Zhang, X.Li, F.Zhu, Y.Liu. *GNSS timing performance assessment and results analysis*. Sensors, 22(7), **2486**, (2022). https://doi.org/10.3390/s22072486

24. M.Ouyang, X.Zhu, J.Li, Y.Liu. *A Modified Single-Frequency PPP Method for the Positioning and Time Transfer with BDS-3*. Sensors. 22(23), **9059**, (2022). https://doi.org/10.3390/s22239059

25. N.Boguspayev, D.Akhmedov, A.Raskaliyev, A.Kim, A.Sukhenko. *A comprehensive review of GNSS/INS integration techniques for land and air vehicle applications*. Applied Sciences. 13(8), **4819**, (2023). https://doi.org/10.3390/app13084819

26. E.Gill, J.Morton, P.Axelrad, D.M.Akos, M.Centrella, S.Speretta. *Overview of space-capable global navigation satellite systems receivers: heritage, status and the trend towards miniaturization*. Sensors, 23(17), (2023). P.7648. https://doi.org/10.3390/s23177648

27. P.Pintor, E.González, A.Senado, P.Bohlig, A.Sperl, P.Henkel, ... J.Vázquez. *Galileo high accuracy service (HAS) algorithm and receiver development and testing*. In Proceedings of the 35th International Technical Meeting of the Satellite Division of The Institute of Navigation (ION GNSS+2022). (2022), P.836-851. https://doi.org/10.33012/2022.18462

28. H.Lee, J.Tak. *Wearable antenna integrated into military berets for indoor/outdoor positioning system*. IEEE Antennas and Wireless Propagation Letters, 16, (2017). pp.1919-1922. DOI 10.1109/LAWP.2017.2688400

29. S.Li, W.Xu, Z.Li. *Review of the SBAS InSAR Time-series algorithms, applications, and challenges*. Geodesy and Geodynamics, 13(2), (2022). pp.114-126. https://doi.org/10.1016/j.geog.2021.09.007

30. Z.Zhang, L.Pan. *Current performance of open position service with almost fully deployed multi-GNSS constellations: GPS, GLONASS, Galileo, BDS-2, and BDS-3*. Advances in Space Research, 69(5), (2022). 1994-2019. https://doi.org/10.1016/j.asr.2021.12.002

31. P.Steigenberger, O.Montenbruck, A.Hauschild. *Antenna and attitude modeling of modernized GLONASS satellites*. Advances in Space Research, 74(7), (2024). pp.3045-3059. https://doi.org/10.1016/j.asr.2024.07.001

32. X.Li, J.Lou, Y.Yuan, J.Wu, K.Zhang. *Determination of global geodetic parameters using satellite laser ranging to Galileo, GLONASS, and BeiDou satellites*. Satellite Navigation, 5(1), (2024). P.10. https://doi.org/10.1186/s43020-024-00132-x

33. S.Karutin. *GLONASS: The Decade of Transition to CDMA Signals*. GPS World, 34(12), (2023). P.39. https://link.gale.com/apps/doc/A779131187/AONE?u=anon~f06e1d0d&sid=googleScholar&xid=cbd724be

34. S.Zaminpardaz, P.J.Teunissen, A.Khodabandeh. *GLONASS-only FDMA+CDMA RTK: performance and outlook*. GPS Solutions, 25(3), (2021). 96. https://doi.org/10.1007/s10291-021-01132-z

35. A.Rachman, A.Vananti, T.Schildknecht. *Spin Period Evolution of Decommissioned GLONASS Satellites*. Aerospace, 12(4), (2025). P.283. https://doi.org/10.3390/aerospace12040283

36. K.Krasuski, M.Mrozik, D.Wierzbicki, J.Ćwiklak, J.Kozuba, A.Ciećko. *Designation of the quality of EGNOS+SDCM satellite positioning in the approach to landing procedure*. Applied Sciences, 12(3), (2022). P.1335. https://doi.org/10.3390/app12031335

37. F.Diani, F.Sbardellati, M Lisi. *GNSS user technology: Next generation GNSS-based location technologies*. In 2019 European Microwave Conference in Central Europe (EuMCE) (2019). pp.319-322. IEEE. https://ieeexplore.ieee.org/abstract/document/8874763

38. P.F.Bakker, C.C.Tiberius. *Real-time multi-GNSS single-frequency precise point positioning*. GPS Solutions, 21(4), (2017). 1791-1803. https://doi.org/10.1007/s10291-017-0653-2

39. S.Chuang, Y.Wenting, S.Weiwei, L.Yidong, Y.Yibin, Z.Rui. *GLONASS pseudorange inter-channel biases and their effects on combined GPS/GLONASS precise point positioning*. GPS solutions, 17(4), (2013). pp.439-451. https://doi.org/10.1007/s10291-013-0332-x

40. K.Špoljar, M.Zrinjski, A.Tupek, K.Stipetić. *Modernization of GNSS, RNSS, and SBAS*. Technologies, 13(11), (2025). P.494. https://doi.org/10.3390/technologies13110494

41. A.Kuttybayeva, et al. *Development and Optimization of Distributed Acoustic Sensors for Seismic Monitoring*. 2024 International Conference on Electrical Engineering and Photonics (EExPolytech). IEEE, (2024). pp.64-67. **DOI:** 10.1109/EExPolytech62224.2024.10755702

42. A.Kuttybayeva, et al. *Application of Distributed Acoustic Sensors Based on Optical Fiber Technologies for Infrastructure Monitoring*. 2024 International Conference on Electrical Engineering and Photonics (EExPolytech). IEEE, (2024). pp.23-26. **DOI:** 10.1109/EExPolytech62224.2024.10755937

43. A.Abdykadyrov, et al. *Optimization of distributed acoustic sensors based on fiber optic technologies*. Eastern-European Journal of Enterprise Technologies. V.131, №5, (2024). DOI: 10.15587/1729-4061.2024.313455

44. G.B.Tolen, et al. *Influence of external factors on power transmission in few-mode optical fiber transmission lines*. Optical Technologies for Telecommunications 2024. **13738**, (2025). pp.120-129. DOI: 10.1117/12.3067490

45. G.B.Tolen, et al. *Analysis of the efficiency of distributed fiber optic acoustic sensors in monitoring systems*. Optical Technologies for Telecommunications 2024. **13738**, (2025). pp.111-119. DOI: 10.1117/12.3067489

46. A.S.Evtushenko, et al. *Simulation of laser-excited optical pulse propagation over graded-index multimode optical fiber with distorted asymmetrical structure*. Optical Technologies for Telecommunications 2024. **13738**, (2025). pp.167-178. DOI: 10.1117/12.3067570

47. G.B.Tolen, et al. *Exploring the potentiality application of silica 5-mode optical fiber with perturbed refractive index profile in distributed acoustic sensing*. Optical Technologies for Telecommunications 2024. **13738**, (2025). pp.130-139. DOI: 10.1117/12.3067491

48. E.Yuldashev, M.Yuldasheva, A.Togayev, J.Abdullayev, R.Karimov. *Energy efficiency research of conveyor transport*. AIP Conference Proceedings, 3331(1), **040030**, (2025), https://doi.org/10.1063/5.0305742

49. A.Abdykadyrov, et al. *Mechanisms of signal loss and reflection in optical fibers and their impact on radio direction finding efficiency in bent cable routes*. International Journal of Innovative Research and Scientific Studies, 8(3), (2025), pp.5056-5069. DOI: 10.53894/IJIRSS.V8I3.7706

50. A.Sabibolda, et al. *Estimation of the Time Efficiency of a Radio Direction Finder Operating on the Basis of a Searchless Spectral Method of Dispersion-Correlation Radio Direction Finding*. Mechanisms and Machine Science, 167 MMS, (2024), pp.62-70. DOI: 10.1007/978-3-031-67569-0_8

51. N.Smailov, et al. *Fiber laser-based two-wavelength sensors for detecting temperature and strain on concrete structures*. International Journal of Innovative Research and Scientific Studies, 7(4), (2024), pp.1693-1710. DOI: 10.53894/ijirss.v7i4.3481

52. N.Smailov, et al. *Streamlining digital correlation-interferometric direction finding with spatial analytical signal | usprawnienie cyfrowego korelacyjno-interferometrycznego ustalania kierunku za pomocą przestrzennego sygnału analitycznego*. Informatyka Automatyka Pomiary W Gospodarce I Ochronie Srodowiska, 14(3), (2024), pp.43-48. DOI: 10.35784/iapgos.6177

53. N.Smailov, et al. *Improving the accuracy of a digital spectral correlation-interferometric method of direction finding with analytical signal reconstruction for processing an incomplete spectrum of the signal*. Eastern European Journal of Enterprise Technologies, 5(9(125)), (2023), pp.14-25. DOI: 10.15587/1729-4061.2023.288397

54. A.Sabibolda, et al. I*mproving the accuracy and performance speed of the digital spectralcorrelation method for measuring delay in radio signals and direction finding*. Eastern European Journal of Enterprise Technologies, 1(9-115), (2022), pp.6-14. DOI: 10.15587/1729-4061.2022.252561

55. M.Sadullaev, E.Usmanov, R.Karimov, D.Xushvaktov, D.Xalmanov, Y.Shoyimov, D.Khimmataliev. *Mathematical Models and Calculation of Elements of Developed Schemes of Contactless Devices*. AIP Conference Proceedings, 3331(1), **040043**, (2025), https://doi.org/10.1063/5.0305748

56. A.Abdykadyrov, et al. *Development and evaluation of radio frequency management approaches for stratospheric communication systems*. Eastern European Journal of Enterprise Technologies, 3(5), (2025), pp.17-29. DOI: 10.15587/1729-4061.2025.331607

57. A.Nuraliyev, I.Jalolov, M.Peysenov, A.Adxamov, S.Rismukhamedov, R.Karimov. *Improving and Increasing the Efficiency of the Industrial Gas Waste Cleaning Electrical Filter Device*. AIP Conference Proceedings, 3331(1), **040040**, (2025), https://doi.org/10.1063/5.0305751

58. M.Sadullaev, E.Usmanov, R.Karimov, D.Xushvaktov, N.Tairova, A.Yusubaliev. *Development of Contactless Device Schemes for Automatic Control of the Power of a Capacitor Battery*. AIP Conference Proceedings, 3331(1), **040042**, (2025), https://doi.org/10.1063/5.0305879

59. M.Sadullaev, E.Usmanov, R.Karimov, D.Xushvaktov, N.Tairova, A.Yusubaliev. *Review of Literature Sources and Internet Materials on Contactless Devices for Reactive Power Compensation*. AIP Conference Proceedings, 3331(1), **040041**, (2025), https://doi.org/10.1063/5.0305878

60. M.Sadullaev, M.Bobojanov, R.Karimov, D.Xushvaktov, Y.Shoyimov, H.Achilov. *Experimental Studies of Contactless Devices for Controlling the Power of Capacitor Batteries*. AIP Conference Proceedings, 3331(1), **040044**, (2025), https://doi.org/10.1063/5.0307195

61. E.Usmanov, M.Bobojanov, R.Karimov, D.Xalmanov, N.Tairova, S.Torayev. *Contactless Switching Devices Using Nonlinear Circuits*. AIP Conference Proceedings, 3331(1), **040031**, (2025), https://doi.org/10.1063/5.0305744

62. Y.Adilov, A.Nuraliyev, M.Abdullayev, S.Matkarimov. *Dynamic Performance Model of a Hybrid Power System*. AIP Conference Proceedings, 3331(1), **040038**, (2025). https://doi.org/10.1063/5.0305909

63. Y.Adilov, M.Khabibullaev. *Application of fiber-optic measuring current transformer in control and relay protection systems of belt conveyor drives*. IOP Conference Series Earth and Environmental Science, 614(1), **012022**, (2020), doi:10.1088/1755-1315/614/1/012022

64. K.Abidov, A.Alimov, M.Gafurova. *Transients in Devices of Control Systems With Excitation Winding*. AIP Conference Proceedings, 3331(1), **040033**, (2025), https://doi.org/10.1063/5.0305756

65. K.Abidov, E.Abduraimov, M.Gafurova. *Possibility of Applying Methods of Analysis and Synthesis of Linear Electrical Circuits to Some Nonlinear Circuits*. AIP Conference Proceedings, 3331(1), **040034**, (2025), https://doi.org/10.1063/5.0305757

66. D.S.Rumi, S.Zh.Nimatov, I.A.Garafutdinova, B.G.Atabaev, S.V.Shevelev. *The investigation of the structure and anisotropy of emission characteristics of (111) zone of a cylindrical tungsten single crystal*. Surface Investigation X Ray Synchrotron and Neutron Techniques, 16(6), (2001), pp.941-948.